

Chapter 13

Performance-Based Seismic Design of RC Structures



Payal Gwalani and Yogendra Singh

Abstract The concept of performance-based design (PBD) is to achieve the design of structures with a reliable understanding of the risk to life and accompanied losses that may occur due to future earthquakes. The design methodology is based on the assessment of a building's performance to determine its probability of experiencing different types of damage levels, considering a range of potential earthquakes that may affect the building structure. The performance objectives (or damage levels) such as immediate occupancy, life safety, or collapse prevention are used to define the damage state of the building. Thus, the methodology enables the owner with a means to select the desired performance goal of the building. The Indian seismic design code (IS 1893 Part 1 [6]), like most other national codes worldwide, provides simplified guidelines for the design of buildings intended to provide life safety performance level of the building against a design level earthquake. However, the prescriptive nature of these guidelines does not provide any framework to estimate the actual intended/expected seismic performance of such buildings. This article describes the technical basis of PBD and its application to building archetypes of moment frame and frame-shear wall buildings. The buildings are designed using the hazard and member design procedures of the relevant Indian codes.

13.1 Introduction

The performance of a building during an earthquake event is highly uncertain and is dependent on many factors (seismic source properties, intensity of ground motion, selection of structural system, configuration and proportion, quality of construction, reinforcement detailing, building maintenance, etc.). The effect of some of these parameters (selection of structural system, configuration and proportion, and reinforcement detailing) can be evaluated and controlled at the design stage. For this, different countries have developed seismic design guidelines based on the knowledge

P. Gwalani · Y. Singh (✉)

Department of Earthquake Engineering, IIT Roorkee, Roorkee, India

e-mail: yogendra.singh@eq.iitr.ac.in

© Indian Society of Earthquake Technology 2023

T. G. Sitharam et al. (eds.), *Theory and Practice in Earthquake Engineering*

and Technology, Springer Tracts in Civil Engineering,

https://doi.org/10.1007/978-981-19-2324-1_13

of the severity of earthquakes and structure's performance in the past events. The current guidelines in the seismic design codes, world-over, are traditionally based on the concept of force-based design. In this approach, each individual member of the structural system is proportioned for strength on the basis of internal forces developed during an elastic analysis. The inelasticity in the structure is incorporated by the use of 'response reduction factor' or 'behaviour factor', adopted based on some presumed inelastic energy dissipation capacity of the structure. The impact of building damage post-earthquake is accounted for by the use of 'importance factor'.

An effective interpretation and characterization of the damage, which occurred in the buildings during past earthquakes (in the mid and late twentieth century), revealed that the traditional seismic design methods could not efficaciously ensure the expected performance of buildings during such events [31]. The use of yielding strength (force) as the basis for design is not efficient enough, as there is no clear relation between strength and damage [29, 30]. To overcome the limitations imposed by the forced-based design methodology, an alternative design philosophy named 'Displacement-based design (DBD)' (Qi and Moehle [32]) was introduced, wherein, translational displacement, rotation, strain, etc. are included in the basic design criterion. A major development in this regard has been made by Priestley [30] and his group [31] in developing a practical methodology for DBD. In this approach, the inter-storey drifts and ductility demand are considered as governing parameters for ensuring the desired performance.

With the advancements in the field of earthquake engineering, FEMA 273 [14] introduced a new concept of seismic design, known as performance-based design (PBD), which enables the designer to design a structure for any targeted performance level. Buildings designed according to the current seismic design codes are intended to sustain some damage under a 'design level' earthquake and follow a 'No collapse' criterion for major earthquakes. However, the prescriptive nature of the code guidelines does not provide any framework for estimation of the actual intended/expected seismic performance of such buildings. On the contrary, PBD is a tool that allows the owner to set the intended performance objective (acceptable damage level) of the buildings. In PBD procedure, a realistic estimate of strength and ductility of the structural system is estimated, with the explicit consideration of non-linear deformation of the members. The performance objectives (or damage levels) are determined in terms of limits on the inelastic deformation of members (instead of force as a damage indicator in force-based design). A non-linear static analysis is imperative for such evaluation. Using this framework, the damage levels of the building can be used to estimate the potential casualties and accompanied losses using some empirical relations.

In the past two decades, the PBD procedure has undergone a significant development (FEMA 356 [15], FEMA 440 [16] ASCE 41-17 [3]) and has adopted a probabilistic framework in the last few years (FEMA P695 [17], FEMA P58 [18], FEMA P58 [19]). In its seminal form, the design methodology is based on the assessment of a building's performance to determine its probability of experiencing different types of damage levels by considering a suite of potential earthquake ground motions that may affect the building structure in future. This article provides guidance to the

design professionals and individuals on the implementation of performance-based seismic design of buildings, in conjunction with the Indian codes of practice. To illustrate this, two structural systems, a moment frame building and a frame-shear wall building are considered. These buildings are designed and detailed using the current Indian seismic design codes IS 1893 Part 1 [6] and IS 13920 [5]. The seismic performance of these buildings is evaluated using non-linear static and dynamic analysis. The building models are developed and analyzed using the commercial software ETABS (CSI [11]), which is commonly used in the design offices in India.

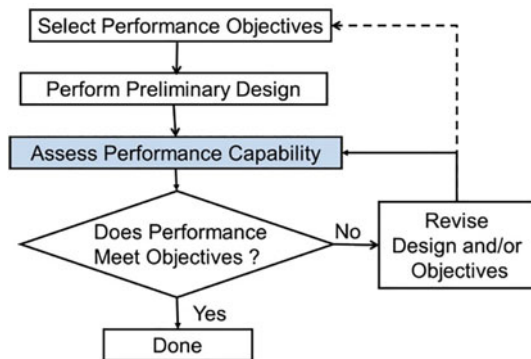
13.2 PBD Procedure

In this study, the methodology to evaluate the performance of building models is separated into five stages: 1. Assessment and representation of ground shaking hazard, 2. Selection of performance objective(s), 3. Structural modelling of the building, 4. Non-linear analysis, and 5. Assessment of performance and iterative revision of design. A brief description of each of these stages is presented here. The process of performance-based design is briefly summarized in Fig. 13.1.

13.2.1 Assessment and Representation of Ground Shaking Hazard

Ground shaking hazard is specified in different ways depending on the type of non-linear analysis method used to quantify the building response. The PBD procedure involves defining the performance objectives in terms of performance levels of the building corresponding to different hazard levels. The hazard levels are represented in terms of the probability of occurrence of the specified intensity in the design life (usually 50 years). Two hazard levels—representing intensities corresponding to 10%

Fig. 13.1 Flowchart of the performance-based design process (FEMA P58 [18])



probability of exceedance in 50 years (termed as Design Basis Earthquake, DBE) and 2% probability of exceedance in 50 years (termed as Maximum Considered Earthquake, MCE)—are most commonly used across the world. Depending on the type of analysis, the ground shaking intensity corresponding to a chosen hazard level is represented by either a 5% damped elastic response spectrum (uniform hazard spectrum corresponding to a given probability of occurrence) or by a suite of ground motions, which have to be carefully selected and scaled to represent the chosen intensity.

13.2.2 Selection of Performance Objective(s)

A performance objective is the means to quantify the building’s performance in terms that will be useful to the owner/designer to make the decision. ASCE 41-17 [3] defines discrete performance levels to evaluate the response of the building. These performance levels, namely, (Fig. 13.2) Operational (O), Immediate Occupancy (IO), Life safety (LS), and/or collapse prevention (CP), are defined by an appropriate acceptable range of strength and deformation demands on the structural and non-structural components of the structural system. The structural damage is represented by the inelastic rotation and deformation, while the non-structural damage is associated with the peak floor acceleration and inter-storey drift. These performance objectives are then utilized to estimate the probable losses to life, economy, and other physical losses to infrastructure/ community, using empirical relations. Table 13.1 summarizes different performance levels used in the literature.

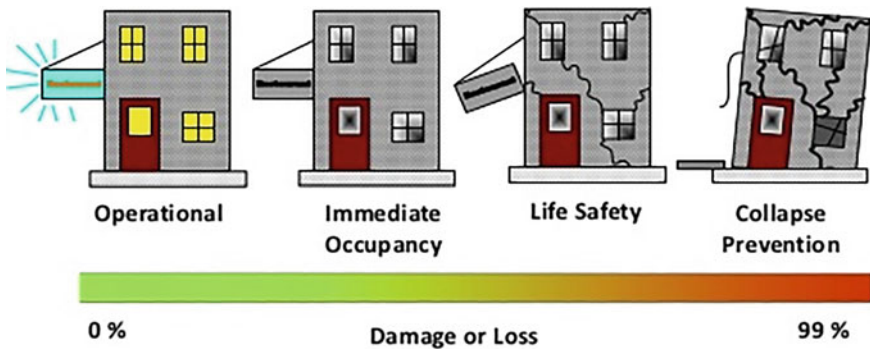


Fig. 13.2 Performance levels in performance-based design (NEHRP [25])

Table 13.1 Different performance levels considered in the literature

Document	Performance Levels	
	Structural	Non-structural
Vision 2000 (SEAOC [35])	Fully Operational Operational Life Safe Near Collapse	
SEAOC [37]	SP1, Operational SP2, Occupiable SP3, Life Safe SP4, Near Collapse SP5, Collapsed	NP1 (Damage Ratio 0%–10%) NP2 (Damage Ratio 5%–30%) NP3 (Damage Ratio 20%–50%) NP4 (Damage Ratio 40%–80%) NP5 (Damage Ratio >70%)
ATC 40 [4]	SP-1, Immediate Occupancy SP-2, Damage Control SP-3, Life Safety SP-4, Limited Safety SP-5, Structural Stability SP-6, Not Considered	NP-A, Operational NP-B, Immediate Occupancy NP-C, Life Safety NP-D, Hazard Reduced NP-E, Not Considered
BS EN 1998-3: [13]	Damage Limitation (DL) Significant Damage (SD) Near Collapse (NC)	
TSC [39]	Ready For Use Life Safety Pre-collapse Collapse	
Model Code for DBSD (Calvi and Sullivan [7])	Level 1, Serviceability Level 2, Damage Control Level 3, Collapse Prevention	
ASCE 41-17 [3]	S-1, Immediate Occupancy S-2, Damage Control (Range) S-3, Life Safety S-4, Limited Safety (Range) S-5, Collapse Prevention S-6, Not Considered	N-A, Operational N-B, Immediate Occupancy N-C, Life Safety N-D, Hazard Reduced N-E, Not Considered

13.2.3 Structural Modelling

It is to be noted that a building has some over-strength, over and above its design strength, due to the use of characteristic strength (95% confidence level) and partial safety factors in loads and materials. Hence, the actual expected strength of the building during an earthquake event is higher than the calculated design strength. Performance assessment of building structures involves evaluating the non-linear response of the structural model considering its expected strength (with the value of partial safety factors = 1). In order to evaluate the non-linear behaviour of a building

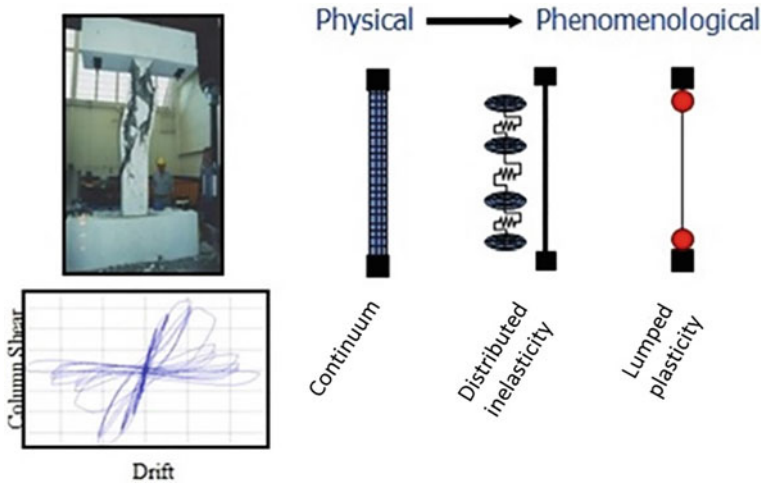


Fig. 13.3 Comparison of non-linear modelling approaches (PEER ATC-72-1) [27]

during a cyclic loading event, it becomes necessary to develop modelling strategies that can incorporate all modes that lead to the deterioration of the structural members. Three modelling approaches with different levels of accuracy and complexity are available in the literature: (i) Continuum model, (ii) Distributed inelasticity model, and (iii) Lumped plasticity model. Figure 13.3 illustrates the modelling strategy in the three different non-linear models.

In Continuum modelling, the non-linear behaviour of the structural members is evaluated by using finite element meshing throughout the section and length of the members to represent both concrete and steel reinforcement bars. The use of such explicit finite element models is mainly limited to detailed analysis of isolated critical elements (such as beam–column joints, etc.) due to its high complexity, time consumption, and computational cost.

In distributed inelasticity model, several cross-sections with finite length are considered throughout the length of the member. At these cross sections, the non-linearity of the member is studied by discretizing the section into several fibres of confined and unconfined concrete and reinforcing steel bar. Each fibre in the cross section is assigned the corresponding material stress–strain relationship. The number of fibre cross-sections and their location is determined by the numerical integration rule, which implicitly defines the plastic hinge length over which the inelasticity of the element can occur. This model has an advantage over lumped plasticity model as it does not restrict the inelasticity at the ends of the element, but it still requires a very large computational capacity and computation time (though less than continuum models). Also, it is difficult to account for flexural–shear interaction, bond-slip, and rebar buckling and fracture using typically distributed plasticity models. However, current research is widely based on resolving these issues [8, 9, 22, 24, 28, 33], but

their application is limited, in particular reference to its implementation in available commercial software packages.

Fibre elements are modelled using two different finite element approaches, namely, displacement-based approach (e.g., Zeris and Mahin [40]) and force-based approach (e.g., Neuenhofer and Filippou [26], Spacone et al. [36]). The displacement-based fibre element (DB) is based on the element's stiffness, while the force-based fibre element (FB) is based on the element's flexibility. In DB element, displacement interpolation functions are used, i.e., cubic and linear shape functions, respectively, for the transverse and axial displacements. These assumed shape functions are approximate representations of the actual displacement, and therefore, a number of elements in a structural member are required to obtain the actual response [10]. These functions are then used to determine the element displacement field by interpolating the nodal displacements. Strain at any point in the cross section is determined by nodal displacements. The stresses are then obtained from the strains using the material stress–strain relationship. This approach has the limitation that the element behaviour is characterized by linear curvature and constant axial strain fields. The non-linear curvature behaviour cannot be represented accurately. Also, the equilibrium condition in each section may not be satisfied.

In force-based fibre element, force interpolation functions (shape functions) are used to determine the section deformations. Strain in the cross section is obtained based on plane section remains plane assumption. Stress and stiffness are obtained from strains using the material stress–strain relationship. The section resisting forces are computed from the fibre stress distribution, and the stiffness matrix is obtained from the fibre stiffness. The FB elements have an advantage over DB elements, in that, the non-linear behaviour of members can be modelled using a single element. This is because the force field gives the exact solution of the governing equilibrium equations irrespective of the occurrence of plastic deformations.

In lumped plasticity model, an elastic line element is used to simulate the behaviour of the member, while yielding is assumed to take place at generalized plastic hinges of zero-length at the ends or other potential plastic hinge locations in a member. The plastic hinge modelling assumption reduces the computational demand and provides a balance between accuracy and complexity level. These models can be easily used to calibrate and capture the observed non-linear behaviour of RC members, i.e., from the start of yielding to the residual strength, including strength and stiffness degradation from concrete crushing and spalling, rebar buckling and fracture, and bond-slip. The non-linearity in lumped plasticity models can be considered by using either of the two hinge models, namely, moment-rotation hinge and fibre-hinge.

The moment-rotation hinge models are based on the definition of phenomenological relation of the overall force–deformation response or moment-rotation (curvature) of structural members (beam, column, shear wall), as observed from the experimental test results (PEER ATC-72-1 [27]). Based on various experimental results on the cyclic behaviour of beam–column elements, various documents have proposed the force–deformation cyclic backbone curves [3, 15, 21]. Figure 13.4 shows the backbone curve as defined in ASCE 41-17 [3]. The first branch of the backbone

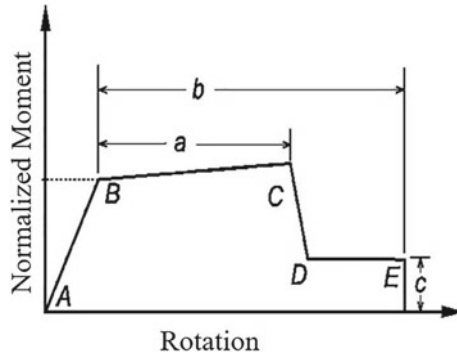


Fig. 13.4 Force–deformation curve (backbone curve) for frame elements in flexure [3]

curve (AB) represents the elastic behaviour of the member, the second branch (BC) represents the post-yield behaviour of the member, and the third branch (CDE) represents the post-peak behaviour of the member, where the strength of the member drops due to strain softening and rebar buckling.

In the fibre-hinge model, fibre-monitoring cross sections are considered at the plastic hinge locations, where the non-linearity of the member is assumed to be lumped. The discretization of monitored sections (into fibres of confined and unconfined concrete and rebars) yields an accurate response by obtaining the P-M and P-M-M interaction of beams and columns, respectively, directly by integration of the inelastic material response. The plastic hinge length for fibre-hinge is obtained from empirical relations derived from experimental test results. Figure 13.5 shows a typical discretization pattern of cross section at the fibre-hinge. The stress–strain curve of concrete should account for the effect of confinement caused by the transverse reinforcement. The cyclic response of materials can be modelled using a suitable hysteresis model duly calibrated with relevant laboratory test data.

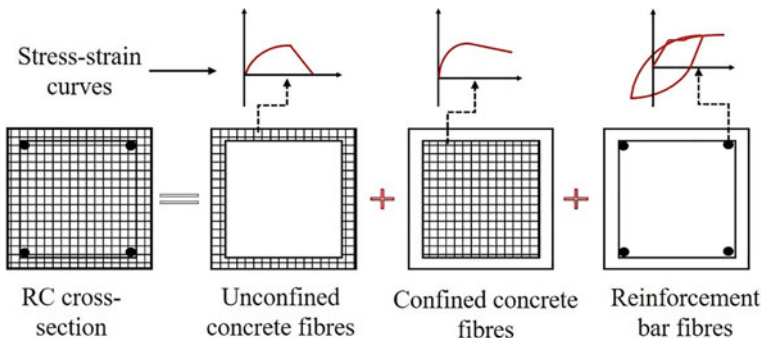


Fig. 13.5 Typical discretization pattern of a RC cross section at the fibre-hinge

13.2.4 Non-linear Analysis

In order to achieve the targeted performance objectives, PBD procedure involves estimation of the performance level of the structure. The performance of the structure can be estimated using either non-linear static analysis or non-linear dynamic analysis.

In non-linear static analysis (NSA), the capacity curve (popularly known as ‘pushover curve’) of the building, which represents the plot between the base shear and roof displacement, is obtained under an assumed distribution of lateral load. The lateral load distribution is considered as an approximate representation of the inertial forces developed in the structure under an actual earthquake loading event. The magnitude of the lateral load is increased monotonically to identify the critical sections (or weak links) of the building and study the failure mode. The accuracy of the pushover analysis depends upon the selection of an ideal lateral load distribution pattern (that can consider the fundamental and higher mode effects). It is a simplified method that provides useful information on the yield strength, failure mechanism, and ductility of the structure. Due to these reasons, design engineers prefer to use the pushover analysis method. However, the method is highly dependent on the loading vector and does not account for the record-to-record variability in the ground motion. Also, the method does not incorporate the biaxial effects of loading and torsional response.

The new generation performance-based design recommends the evaluation of building performance using non-linear dynamic analysis. The method provides a more accurate estimate of structural behaviour (compared to pushover analysis) since the response is obtained by direct application of earthquake ground motion. Due to the inherent variability in the nature of earthquake ground motions, NLTHA is carried out for multiple ground motions to obtain a statistically robust output. ASCE 7-16 [2] recommends a minimum no. of 11 pairs of ground motion (i.e., a 22 GM record set, having two orthogonal components of motion) for NLTHA. The selected ground motions should be representatives of the events with the same tectonic regime, consistent magnitudes, and rupture characteristics as the events that dominate the target response spectrum. Also, ground motions should match the spectral shape of the target spectrum in the range of $0.2 T_L - 2 T_U$, where T_L and T_U are the smaller and larger fundamental periods, respectively, in the two orthogonal directions of the building.

13.2.5 Assessment of Performance and Iterative Revision of Design

It is necessary to assess if the designed building meets the performance objectives targeted by the owner. For a building to comply with a chosen performance level, all structural members must satisfy the prescriptive acceptance criteria. For structural

members, where moment-rotation hinge is used to define non-linearity, the acceptable limits are defined in terms of plastic rotation. ASCE 41-17 [3] provides these acceptable plastic rotation limits based on updated and latest experimental test studies. In case if distributed inelasticity model or fibre-hinge lumped plasticity model is used to simulate the non-linear response of RC members, where plastic rotation of members is not directly obtained, the performance can be estimated in terms of material strain in concrete and steel. These strain limits can be obtained from relevant experimental test results and analysis studies. Table 13.2 shows the limit values of strains corresponding to different performance levels taken from the Turkish seismic code [39] for beams and column members. For structural walls modelled, Akelyan et al. [1] recommends that the maximum compressive strain in concrete and the maximum axial tension strain in steel as obtained from distributed inelasticity or fibre-hinge models should not exceed 0.005 and 0.01, respectively. In addition to the member-level acceptance criteria, the global structural performance of RC buildings can also be evaluated in terms of maximum inter-storey drift. Table 13.3 provides the maximum permissible transient and permanent drift limits recommended by FEMA 356 [15].

In case the actual performance of the building does not comply with the targeted objectives, the next step would be to revise the design so as to achieve the target. Once the design is revised, the aforementioned steps are repeated again to assess the

Table 13.2 Acceptance criteria in terms of strain limit values for the concrete and reinforcing steel for distributed plasticity or fibre models for RC beams and columns [39]

Performance level	Strain limit values	
	Concrete	Reinforcement steel
Immediate occupancy (IO)	$\epsilon_{cu} = 0.0035$	$\epsilon_s = 0.010$
Life safety (LS)	$\epsilon_{cg} = 0.0035 + 0.01 (\rho_s / \rho_{sm}) \leq 0.0135$	$\epsilon_s = 0.040$
Collapse prevention (CP)	$\epsilon_{cg} = 0.004 + 0.014 (\rho_s / \rho_{sm}) \leq 0.0180$	$\epsilon_s = 0.050$

Note ϵ_{cu} = ultimate strain in unconfined concrete, ϵ_{cg} = ultimate strain in confined concrete, ϵ_s = strain in reinforcement steel, ρ_s and ρ_{sm} = Volumetric ratio of special seismic hoops and crossties, and transverse reinforcement, respectively

Table 13.3 Acceptance criterion in terms of maximum permissible transient and permanent drifts [15]

Structural system	IDR(%) for performance level					
	IO		LS		CP	
	Tran	Perm	Tran	Perm	Tran	Perm
RC moment frame	1.0	0.0	2.0	1.0	4.0	4.0
RC moment frame with URM infills	0.1	0.0	0.5	0.3	0.6	0.6
RC moment frame with shear wall (Dual system)	0.5	0.0	1.0	0.5	2.0	2.0

performance of the building. Hence, it is an iterative process that is followed till the targeted performance objectives are achieved.

13.3 Design Example

In the present study, two RC building models with different structural configurations, i.e., one with a moment frame and another one with frame-shear wall are designed to illustrate the above-mentioned PBD procedure. These building models are designed in confirmation with the current Indian seismic design codes—IS 1893 Part 1 [6] and IS 13920 [5]. The results from the present study illustrate the expected performance of the code-complaint buildings for the code-specified earthquake hazard level. The design and analysis of the building models are carried out in the commercial building design software ETABS 2016 [11].

13.3.1 Building Model Description

General Properties

Two 8-storey RC building models i.e., a moment frame and a frame-shear wall building, with plan dimensions as shown in Fig. 13.6, are considered. Both the models have a constant storey height of 3.3 m and a plinth level of 1.5 m. The general properties of the considered buildings are presented in Table 13.4. The period of vibration (1st and 2nd mode) and the member sizes for the considered building models are presented in Table 13.5.

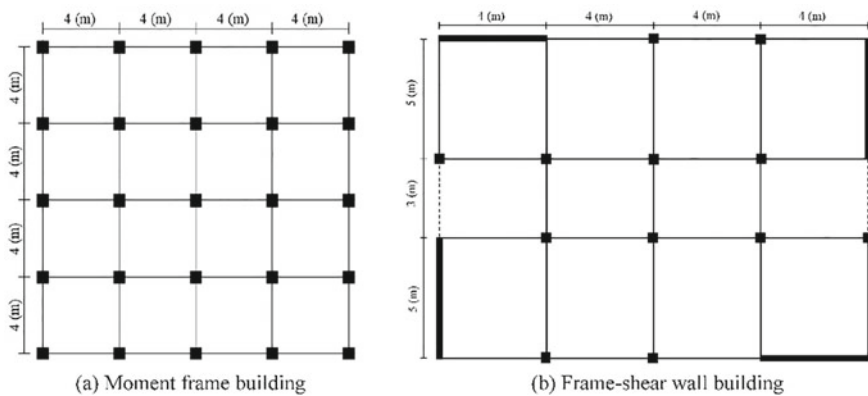


Fig. 13.6 Plan and elevation of the building models considered

Table 13.4 General properties of considered buildings

General	Design level	Bare Frame designed for Gravity and Earthquake Loads and detailed as Special Moment Resisting Frame, according to IS 1893 Part 1 [6] and IS 13920 [5] ductile detailing provisions to avoid shear failure and strong column-weak beam ratio greater than 1.4
	No. of storeys	8-storey
	cracked section properties	Considered from ASCE 41-17 [3]
Seismic Hazard	Soil type	Soil Type I (IS: 1893 [6])
	Seismic zone	Seismic Zone V (IS: 1893 [6]) ($EPG_{MCE} = 1.5 \times 0.36 g = 0.54 g$)
Material	Concrete	Nominal (characteristic) cube strength = 40 MPa
	Steel	Nominal (characteristic) Yield Strength = 500 MPa
Loading	Dead load	Self-weight of members Weight of slabs and floor finish Weight of (230 mm exterior and 120 mm interior) infill walls Weight of 1 m high and 115 mm thick masonry parapet wall
	Live load	4 kN/m ² on corridor 3 kN/m ² on other floor areas 1.5 kN/m ² on roof
	Design load combinations	According to Clause 6.3.4.1 of IS 1893 Part 1 [6]
Structural Modelling	Software used	ETABS (CSI [11])
	Structure model	Space frame model
	Element model	3D frame elements for beams and columns Wide column model for shear wall Slabs as rigid diaphragms
	P-delta effects	Considered in analysis and design

Table 13.5 Details and member sizes of the considered building models

Building model	Period of vibration (s)		Member sizes (mm)		
	X	Y	Beam	Column	Shear wall
Moment frame building	2.75	2.75	300 × 400	400 × 400 350 × 350*	–
Frame-shear wall building	1.71	1.64	300 × 400	400 × 400 350 × 350*	5000 × 150 4000 × 150

* Column size reduction after 4th floor

Non-linear Modelling

Before non-linear modelling and analysis of the buildings, the buildings are analyzed using the mode-superposition (response spectrum) method with an appropriate response reduction factor ($R = 5$) as per IS 1893 Part 1 [6]. In analysis, an effective cracked moment of inertia of beam–columns and shear walls is considered. It is important to consider the P-Delta effect and rigid diaphragm action of floor and roof slabs, in the design and analysis. Finite size of beam–column and beam–shear wall joints is also considered in the modelling. The beams, columns, and shear walls are designed as per relevant IS codes, and detailing is performed as per IS 13920 [5] to obtain the details of longitudinal and transverse reinforcement in each member. This information is necessary for assigning the plastic hinges for non-linear analysis.

Lumped plasticity model is used to define the non-linearity in the elements. Uniaxial moment-rotation plastic hinges (M3) are assigned at both ends of the beams (at a relative distance of 0.05 and 0.95). The backbone curve (i.e., force–deformation envelopes of beams) and the acceptable deformation limits for various performance levels (i.e., IO, LS and CP) are obtained from ASCE 41-17 [3]. The cyclic properties of the moment-rotation hinges are modelled using an energy-based degrading hysteresis model [11]. The details of the model can be found in the CSI [11] manual. Further details of the modelling and calibration can be found in Surana et al. [38]. The properties of the model (f_1 , f_2 and s) for ductile beams are taken from Surana et al. [38].

The non-linearity in columns and shear walls is modelled using the fibre-hinge model. The fibre-hinge is assigned at the two ends of the element, located at the midpoint of the plastic hinge length measured from the face of the connecting element. At each plastic hinge location, the section is discretized into fibres for confined concrete, unconfined concrete, and one steel fibre per reinforcing bar. Plastic hinge length for columns is taken as half of the maximum horizontal dimension of the column. Plastic hinge length for the shear wall is taken from the empirical relation given by Priestley et al. [31]. Mander's model [23] is used for defining the stress–strain relationship between confined and unconfined concrete. The stress–strain curve of the steel reinforcing bar is assumed a bilinear elastic–plastic model with kinematic strain-hardening. The performance level (IO, LS, and CP) in case of fibre-hinge model is indicated by the strain in the extreme fibre. These acceptable values of strains corresponding to different performance levels are taken from the Turkish code [39]. The cyclic properties of the materials are modelled using an energy-based degrading hysteresis model [11]. The properties of the energy hysteresis model for concrete and steel have been calibrated for columns and shear walls using the available experimental test results of Rodrigues et al. [34] and Dazio et al. [12], respectively. Figure 13.7 shows the calibrated force–deformation hysteresis curves of column specimen PB01-N09 [34] and shear wall specimen WSH3 [12]. Further details of the calibration process can be found in Gwalani et al. [20].

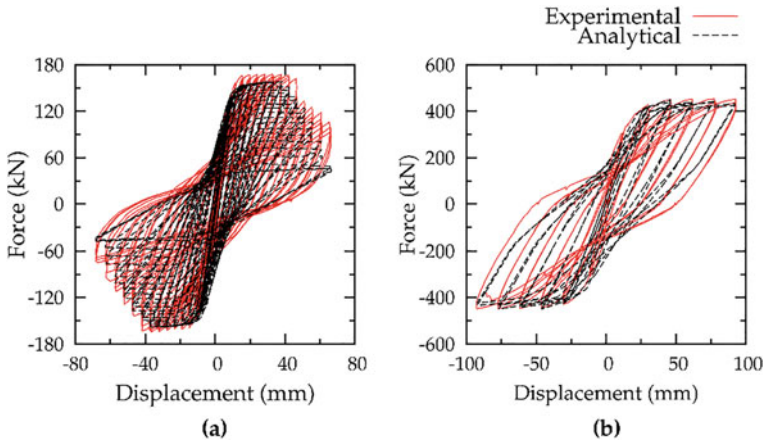


Fig. 13.7 Calibrated force–deformation response using fibre-hinge of: **a** column specimen PB01-N09 [34] and **b** shear wall specimen WSH3 [12]

Non-linear Analysis

In the present study, both Pushover analysis and NLTHA of both the building models are carried out. For the pushover analysis, the lateral load distribution proportional to the fundamental mode of the building is considered. The performance point is computed using the ‘Displacement Modification Method (DMM)’ specified in clause 7.4.3.3 of ASCE 41-17 [3]. For time history analysis of both the buildings, a far-field ground motion with two horizontal components, from FEMA P695 [17] and as shown in Fig. 13.8, is considered. The selected time history is scaled in the time domain (i.e., using a constant scale factor) to have the same spectral acceleration as the MCE response spectrum (corresponding to $1.5 \times Z$) at the fundamental period of the building, and is applied at the base of the building. The roof displacement and hinge pattern are evaluated to compare the results of time history with the pushover analysis. In case of NLTHA, a Rayleigh damping model is used, with a damping ratio of 5% assigned at the fundamental mode and the mode corresponding to 90% of modal mass participation. It is to be noted that as per ASCE 7-16 [2], minimum 11-time histories are to be used to estimate the average response. In the present study, only one-time history has been used for the purpose of illustration only.

13.3.2 Results

13.3.2.1 Moment Frame Building

Figure 13.9 shows the capacity curve obtained from the analysis of the moment frame building. Since it’s a bisymmetric building, both directions have the same pushover

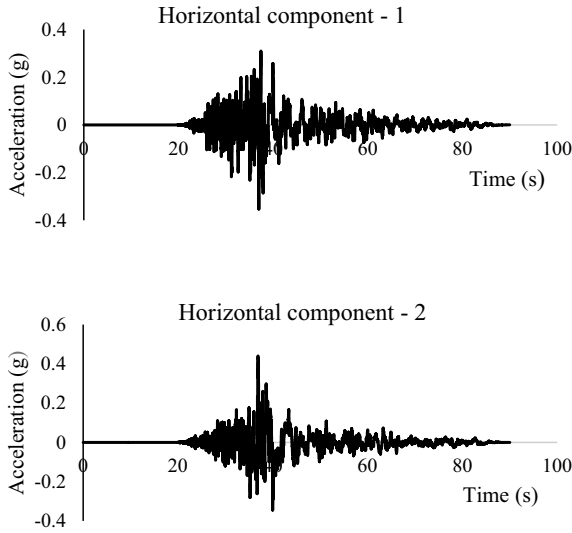


Fig. 13.8 Earthquake ground motion (Chi-Chi, Taiwan earthquake (1999)) considered in NLTHA analysis

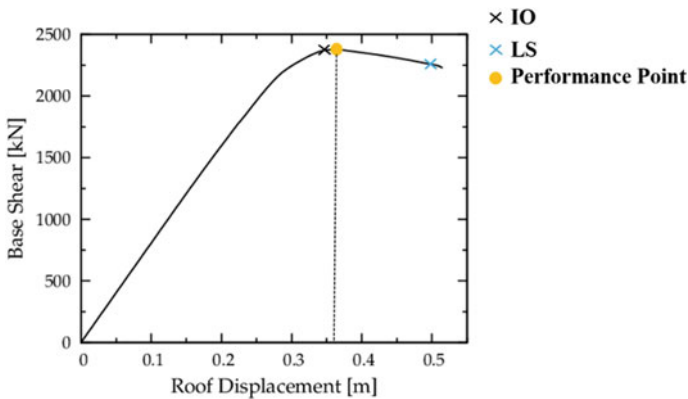


Fig. 13.9 Capacity curve of RC moment frame building obtained from pushover analysis

curve, and only one is shown here. The figure also shows the performance point at MCE and the performance levels IO and LS. The performance levels are obtained from ASCE 41-17 [3]. It is important to note that ASCE 41-17 [3] specifies the acceptable limit of rotation for each individual member, and not for the structural system as a whole. The different performance levels on the capacity curve are marked by identifying the roof displacement corresponding to the pushover step, at which the first member in the building crosses the rotation limit corresponding to the concerned performance level. It is observed that the RC bare moment frame building designed in

confirmation to relevant Indian codes can sustain MCE with LS performance level. This means that the building has sufficient over-strength and ductility to survive, without collapse (in fact with LS level of performance), the MCE ($1.5 \times Z$) level of ground shaking. Figure 13.10a and b show the hinge pattern of the moment frame building at the performance point and at the last step of the pushover curve (failure point). It is observed from the Figures that at the performance point, some beams have hinges that cross the IO performance level, whereas failure of the building occurs due to the formation of beam mechanism (formation of hinges in lower 4-storey beams and formation of hinges in ground storey columns).

Figure 13.11 shows the capacity curve of the building with the performance points obtained from NSA and NLTHA. It can be seen that there is a considerable difference in the roof displacement values obtained from pushover analysis and NLTHA. This difference is due to the fact that pushover is an approximate static analysis method that considers only the fundamental mode of vibration of the building and ignores the dynamic effect of higher modes. Figure 13.12 shows the hinge pattern at the performance point obtained from the NLTHA. A comparison of Figs. 13.10 and 13.12 highlights the difference in the performance of the building obtained using the two analyses. In case of pushover analysis, only a few beams undergo inelastic deformation, whereas a number of members develop plastic hinges in case of NLTHA. Another important observation from the hinge pattern under NLTHA is that even though the building was designed with strong columns and weak beams, with a strength ratio of 1.4, hinges are still formed in some of the columns.

Granted the results presented here are only for a single time history, but it still highlights that the response obtained from pushover analysis is not sufficient enough to adequately judge the performance of the building. A number of time history analyses should also be carried out to reliably estimate the seismic performance of the building.

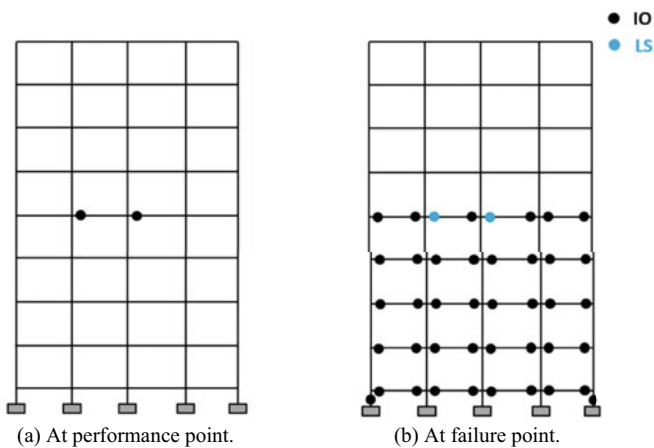


Fig. 13.10 Hinge pattern of RC moment frame building obtained from pushover analysis

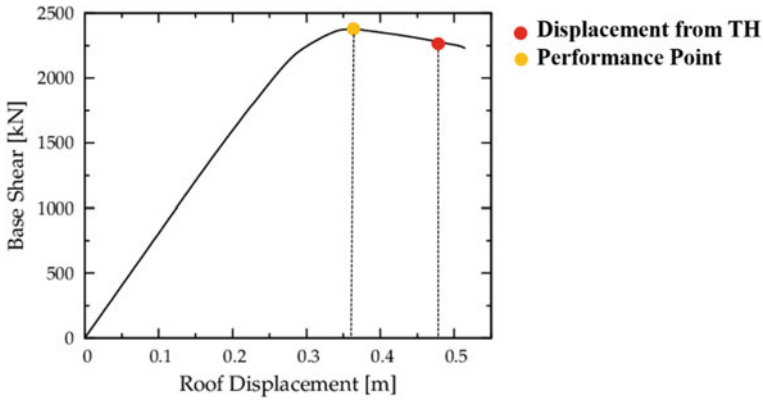
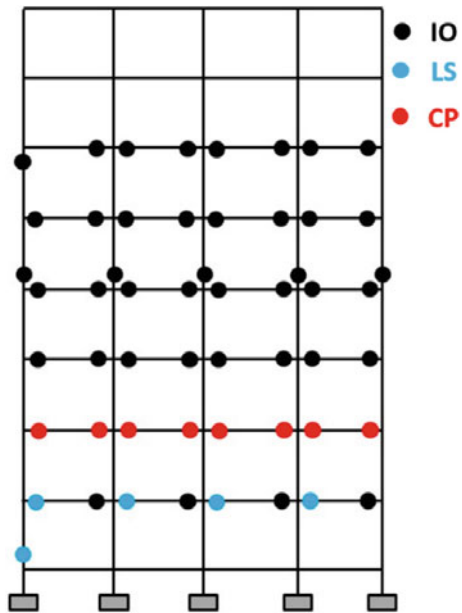


Fig. 13.11 Comparison of performance points obtained from pushover analysis and displacement from time history for RC moment frame

Fig. 13.12 Hinge pattern at Performance Point of RC moment frame building obtained from the non-linear time history analysis (NLTHA)



13.3.2.2 Frame-Shear Wall Building

Figure 13.13 shows the capacity curves obtained from the pushover analysis of the frame-shear wall building in the two directions. Similar to moment frame results, the figure also shows the performance point at MCE and the performance levels IO, LS, and CP. It is observed that frame-shear wall building designed conforming to Indian standard codes also has an LS level performance. The same can be observed

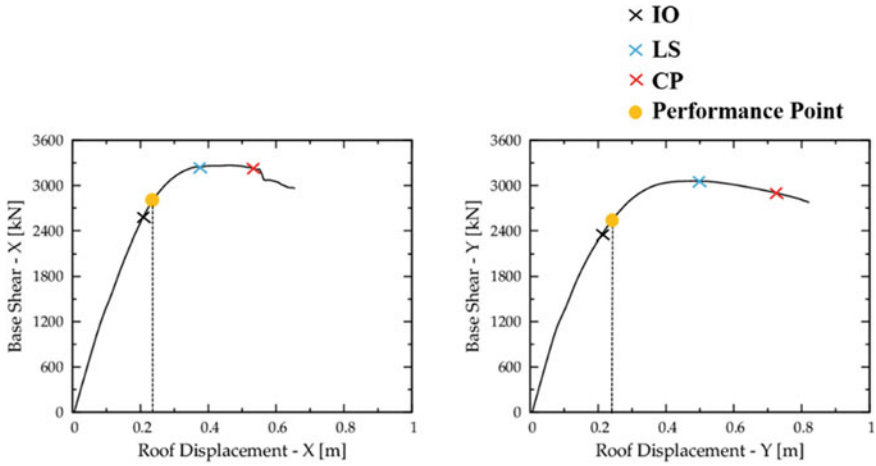


Fig. 13.13 Capacity curve of RC frame-shear wall building obtained from pushover analysis

from the hinge pattern at the performance point shown in Fig. 13.14. The yield in frame-shear wall building starts with hinge formation in the shear wall. Figure 13.15 shows the hinge pattern at the last step of the pushover curve (failure point). It can be observed that failure in case of frame-shear wall building occurs due to the failure of the shear wall (formation of CP hinge in the shear wall). Figure 13.16 shows the capacity curve of the building with the performance point obtained from NSA and

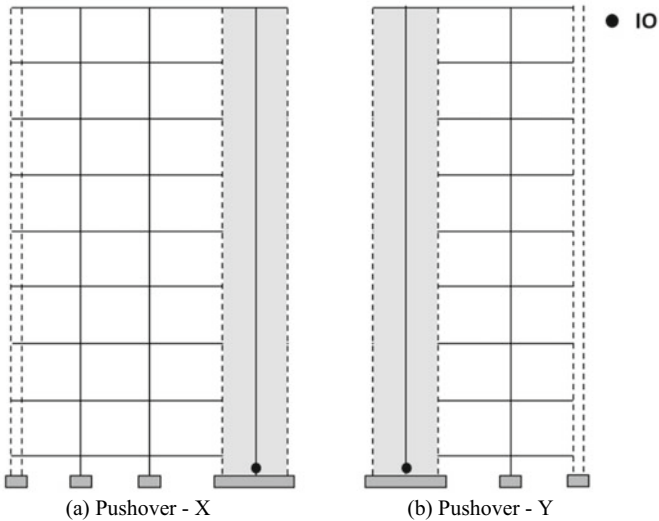


Fig. 13.14 Hinge pattern of RC frame-shear building at performance point obtained from pushover analysis

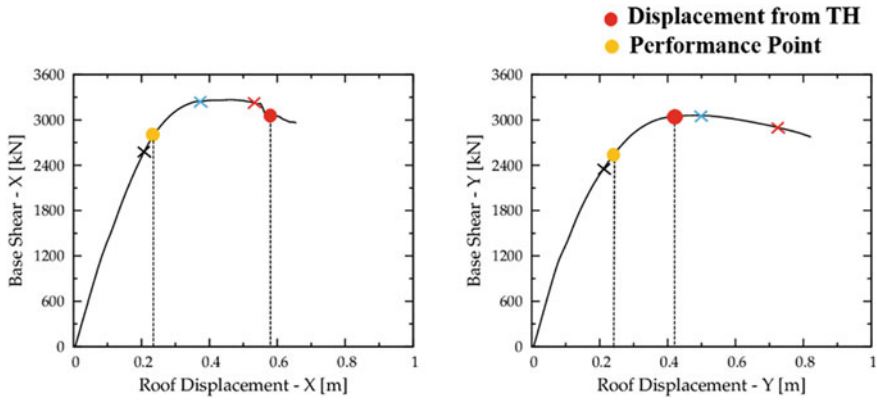


Fig. 13.15 Hinge pattern of the RC frame-shear building at failure point obtained from pushover analysis

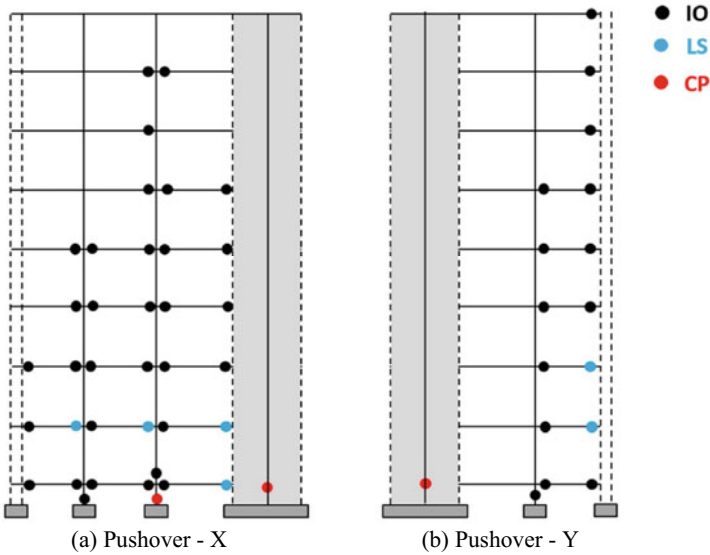


Fig. 13.16 Comparison of performance points obtained from pushover analysis and non-linear time history analysis of the RC frame-shear wall building

the NLTHA. Similar observations as in the case of frame building can be made here as well. Also, the hinge pattern in Fig. 13.17 shows that in case of NLTHA, a larger number of beams show plastic hinges, and many of those show collapse. In this case also, some of the columns develop plastic hinges, even with the strong column-weak beam ratio of 1.40, used in the design.

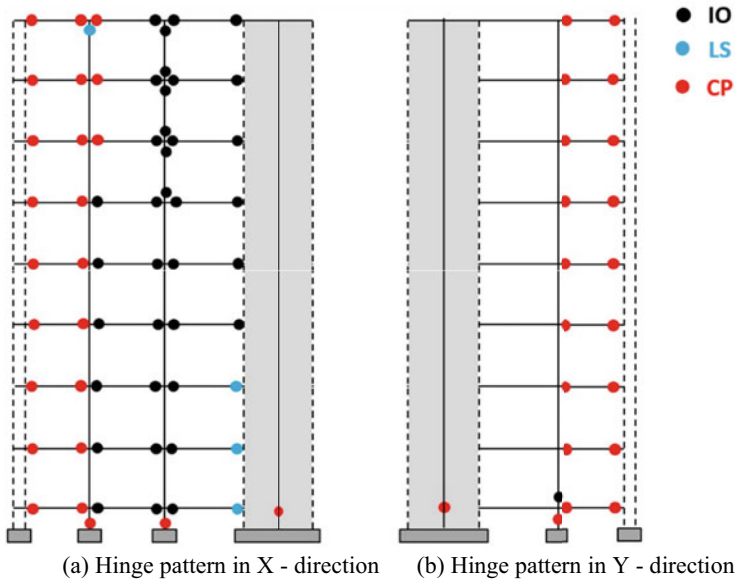


Fig. 13.17 Hinge pattern of the RC frame-shear building obtained from non-linear time history analysis

13.4 Conclusions

An iterative procedure of performance-based design of RC frame and frame-shear wall buildings has been illustrated. The relevant Indian codes have been used to estimate the hazard and design of RC components. The non-linear modelling has been performed considering the modelling and acceptance criteria of ASCE 41-17 [3] and Turkish codes (TSC [39]). The article also provides an idea of the expected performance of the buildings designed using Indian codes. The approach presented is general and is applicable to any type of building. The procedure has been demonstrated through examples of building archetypes of moment frame buildings and frame-shear wall buildings, which are the most common representatives of contemporary buildings in India. A comparison of NSA and NLTHA methods of PBD has shown that the NSA being based on the fundamental mode of structure alone is approximate and may not provide an adequate assessment of expected performance. On the other hand, NLTHA considering the effect of all the modes of vibrations provides an insight into all the possible failure modes of structure, which may not be illustrated by NSA.

References

1. Akelyan MS, Brandow G, Carpenter L, Ekwueme C, Ghodsi MT, Islam S et al. (2020) An alternative procedure for seismic analysis and design of tall buildings located in the Los Angeles region. 2020 Edition, Los Angeles Tall Buildings Structural Design Council
2. ASCE, SEI 7-16 (2016) Minimum design loads for buildings and other structures. American Society of Civil Engineers, Reston
3. ASCE, SEI 41-17 (2017) Seismic rehabilitation of existing buildings. American Society of Civil Engineers, Reston
4. ATC-40 (1996) Seismic evaluation and retrofit of reinforced concrete buildings. Applied Technology Council, Redwood City, California
5. BIS (2016) Ductile design and detailing of reinforced concrete structures subjected to seismic forces – Code of practice – IS 13920. Bureau of Indian Standards, New Delhi
6. BIS (2016b) Indian standard criteria for earthquake resistant design of structures, Part 1: General provisions and buildings (Sixth revision) IS 1893 Part 1. Bureau of Indian Standards, New Delhi
7. Calvi GM, Sullivan TJ (2009) A model code for the displacement-based seismic design of structures. IUSS Press, Pavia
8. Ceresa P, Petrini L, Pinho R (2007) Flexure-shear fiber beam–column elements for modeling frame structures under seismic loading—state of the art. *J Earthq Eng* 11(S1):46–88
9. Ceresa P, Petrini L, Pinho R, Sousa R (2009) A fibre flexure–shear model for seismic analysis of RC-framed structures. *Earthq Eng Struct Dyn* 38(5):565–586
10. Coleman J, Spacone E (2001) Localization issues in force-based frame elements. *J Struct Eng* 127(11):1257–1265
11. CSI (2016) ETABS 2016 Integrated building design software. Version 16.0.1, Computers and Structures Inc., Berkeley, U.S.A
12. Dazio A, Beyer K, Bachmann H (2009) Quasi-static cyclic tests and plastic hinge analysis of RC structural walls. *Eng Struct* 31(7):1556–1571
13. EN 1998-3 EC-8 (2004) Design of structures for earthquake resistance- Part 1: Assessment and retrofitting of buildings. European Committee for Standardization, Brussels
14. FEMA 273 (1997) Guidelines for seismic rehabilitation of buildings. Federal Emergency Management Agency, Washington, D.C., United States
15. FEMA 356 (2000) Prestandard and commentary for the seismic rehabilitation of buildings. Federal Emergency Management Agency, Washington, D.C., United States
16. FEMA 440 (2005) Improvement of inelastic analysis procedures. Federal Emergency Management Agency, Washington, D.C., United States
17. FEMA P695 (2009) Quantification of seismic performance factors. Federal Emergency Management Agency, Washington, D.C., United States
18. FEMA P58 (2012) Seismic performance assessment of buildings -Volume 1 methodology. Federal Emergency Management Agency, Washington, D.C., United States
19. FEMA P58 (2018) Seismic performance assessment of buildings -Volume 1 methodology. Federal Emergency Management Agency, Washington, D.C., United States
20. Gwalani P, Singh Y, Varum H (2021) Effect of proportioning of lateral Stiffness in orthogonal directions on seismic performance of RC buildings. *J Earthq Eng*. <https://doi.org/10.1080/13632469.2021.1964649>
21. Haselton CB, Liel AB, Taylor Lange S, Deierlein GG (2007) Beam column element model calibrated for predicting flexural response leading to global collapse of RC frame building. PEER Report 2007/03, PEER Center, University of California, Berkeley, California, United States
22. Kagermanov A, Ceresa P (2017) Fiber-section model with an exact shear strain profile for two-dimensional RC frame structures. *J Struct Eng* 143(10):04017132
23. Mander JB, Priestley MJ, Park R (1988) Theoretical stress-strain model for confined concrete. *J Struct Eng* 114(8):1804–1826

24. Mergos PE, Kappos AJ (2008) A distributed shear and flexural flexibility model with shear–flexure interaction for R/C members subjected to seismic loading. *Earthq Eng Struct Dyn* 37(12):1349–1370
25. NEHRP FEMA 451B (2006) Recommended provisions: instructional and training materials. Washington DC
26. Neuenhofer A, Filippou FC (1997) Evaluation of nonlinear frame finite-element models. *J Struct Eng* 123(7):958–966
27. PEER / ATC-72-1 (2010) Modelling and acceptance criteria for seismic design and analysis of tall buildings. Applied Technology Council, Redwood City, California, United States
28. Petrangeli M, Pinto PE, Ciampi V (1999) Fiber element for cyclic bending and shear of RC structures. I: Theory. *J Eng Mech* 125(9):994–1001
29. Priestley MJN (1993) Myths and fallacies in earthquake engineering. *Bulletin of NZ Nat Soc for Earthq Eng* 26(3):329341
30. Priestley MJN (2000) Direct displacement based design. Paper presented at 12th Conference on Earthquake Engineering, Auckland, New Zealand, 30 January–4 February 2000
31. Priestley MJN, Calvi GM, Kowalsky MJ (2007) Displacement based seismic design of structures. IUSS Press, Pavia
32. Qi X, Moehle JP (1991) Displacement design approach for reinforced concrete structures subjected to earthquakes, vol UCB/EERC-91/02 Earthquake Engineering Research Center, College of Engineering/University of California
33. Ranzo G, Petrangeli M (1998) A fibre finite beam element with section shear modelling for seismic analysis of RC structures. *J Earthq Eng* 2(03):443–473
34. Rodrigues H, Dias Arede A, Varum H, Costa A (2013) Experimental evaluation of rectangular reinforced concrete column behaviour under biaxial cyclic loading. *Earthq Eng Struct Dyn* 42(2):239–259
35. SEAOC Vision 2000 Committee (1995) Performance-based seismic engineering. Structural Engineers Association of California, Sacramento, California
36. Spacone E, Ciampi V, Filippou FC (1996) Mixed formulation of nonlinear beam finite element. *Comput Struct* 58(1):71–83
37. SEAOC Seismology Committee (1999) Recommended lateral force requirements and commentary. Structural Engineers Association of California, Sacramento, California
38. Surana M, Singh Y, Lang DH (2017) Seismic characterization and vulnerability of building stock in hilly regions. *Nat Haz Rev* 19(1):04017024
39. Turkish Seismic Code (2007) Specifications for buildings to be built in seismic zones. Ministry of Public Work and Settlement Government of Republic of Turkey, Ankara, Turkey
40. Zeris CA, Mahin SA (1988) Analysis of reinforced concrete beam-columns under uniaxial excitation. *J Struct Eng* 114(4):804–820